Fields Institute Communications
Volume **49**, 2006

Mixed Mode Oscillations Due to the Generalized Canard Phenomenon

Morten Brøns
Department of Mathematics
Technical University of Denmark
DK-2800 KGS.Lyngby, Denmark
M.Brons@mat.dtu.dk

Martin Krupa
Department of Mathematical Sciences
New Mexico State University
Las Cruces, NM 88003 USA
mkrupa@nmsu.edu

Martin Wechselberger
School of Mathematics & Statistics
University of Sydney
NSW 2006 Australia
M.Wechselberger@maths.usyd.edu.au

Abstract. Mixed mode oscillations combine features of small oscillations and large oscillations of relaxation type. We describe a mechanism for mixed mode oscillations based on the presence of canard solutions, which are trajectories passing from a stable to an unstable slow manifold. An important ingredient of this mechanism are singularities known as folded nodes. The main focus of this article is to show how the local dynamics near a folded node can combine with global features, leading to mixed mode oscillations. We review and extend the results of [28] on the dynamics near a folded node and state some results on mixed mode periodic orbits with Farey sequences of the form 1^s. We also show how to generalize the context of one fast variable to an arbitrary number of fast variables.

2000 *Mathematics Subject Classification.* Primary ; Secondary.

M. Krupa was supported in part by the National Science Foundation grant No. 0406608 and by the Otto Mønsted Foundation.

Martin Wechselberger was supported in part by the National Science Foundation under Agreement No. 0112050.

1 Introduction

Complex oscillatory behaviour known as mixed mode oscillations (MMO's) were first discovered in the famous Belousov-Zhabotinsky reaction [29]. Since then, MMO's have been frequently observed in both experiments (see e.g. [17, 25, 14, 6, 20]) and models (see e.g. [8, 13, 7, 18, 21]) of chemical and biological systems. The oscillatory behaviour exhibited by these nonlinear systems consists of L large amplitude oscillations followed by s small amplitude oscillations and the symbol L^s is assigned to that pattern. As a function of a control parameter, MMO's often follow bifurcation sequences known as Farey sequences [4]. This ubiquitous behaviour suggests the possibility of the existence of a common dynamical systems theory origin.

Among the proposed mechanisms for MMO's are break-up of an invariant torus [16] and break up/loss of stability of a Shilnikov homoclinic orbit [1, 13]. Both of these scenarios are consistent with the occurence of Farey sequences, but there are certain features of MMO's which cannot be explained. For example the theory of a Shilnikov homoclinic predicts a bifurcation sequence of a growing number of small excursions which has to terminate in the formation of the homoclinic connection corresponding to an infinite amount of small oscillations. However, the most typically observed bifurcation sequences of MMO's are characterized by a bounded number of small oscillations, with the MMO behavior terminating suddenly, without the formation of a homoclinic orbit.

In this paper we present another possible explanation for MMO's. This mechanism is based on a canard phenomenon which can be observed in a 3D framework of slow-fast systems [19, 26, 28]. The classical canard phenomenon (discovered by a group of French mathematicians [2]) occurs in systems with one slow and one fast variable. Its nature is the transition from a small amplitude oscillatory state to a (large amplitude) relaxation oscillatory state within an exponentially small range of the control parameter. This transition, also called *canard explosion*, occurs through a sequence of canard cycles which can be asymptotically stable, but they are very hard to observe in experiment or simulation because of sensitivity to the control parameter and also because of sensitivity to noise. This is well known in the chemical literature where canard explosion is classified as a hard transition, because, for practical purposes, the transition from a small cycle to a relaxation oscillation occurs immediately.

Very important for the understanding of canard explosion is a trajectory called *maximal canard*, which is a connection from the stable slow manifold to the unstable slow manifold. In 2D systems maximal canards occur for discrete values of the control parameter [15], but in 3D maximal canards are robust and are therefore persistent under small parameter changes [26]. It was shown in [28] that a class of canards in 3D called canards of *folded node type* can be responsible for the small amplitude oscillations observed in MMO's. A good intuition is that the system moves dynamically from the excitable state to the oscillatory state and the feature of the large oscillation is to bring the system back to the excitatory state. The number of small oscillations predicted by this canard phenomenon is finite, which is a major difference to the mentioned theory of Shilnikov homoclinic orbit. Furthermore, this canard phenomenon is robust under noise in the sense that many of the deterministically obsrved MMO patterns are preserved.

Another attractive feature of the canard mechanism for MMO's is that, once the slow and the fast variables have been identified, it is very easy to verify if it is the canard based mechanism for MMO's or not. For example, for the systems of [7], [18] and [21, 22] it is known that the MMO mechanism is of canard type.

The main purpose of this work is to explain how MMO's can occur in systems with two slow variables due to the canard phenomenon. We want to point out the main local structure creating the small amplitude oscillations as well as the conditions a global return mechanism must satisfy for MMO's to arise. Furthermore we would like to give some insight to how Farey sequences can be explained by this mechanism. This paper is partly expository and non-technical, but there are more technical parts where we try to explain certain crucial features of the mechanism in quite some detail (in fact the paper does contain some new results). We try to avoid very technical arguments, avoiding the use of the blow-up method, which has been the main technical tool in much of our work. (For an introduction to the use of the blow up method in geometric singular perturbation theory we refer the reader to [15].) Our intention is that this paper should be accessible to anyone familiar with basic dynamical systems and singular perturbation theory, but it should also be useful for people who study MMO's in their research and are not necessarily familiar with the blow-up method.

It is worth mentioning that canard solutions play a fundamental role in other very interesting contexts. Two most notable examples are the dynamics of the forced van der Pol oscillator [10, 3] and a mechanism for localization of oscillation in chemical systems [22, 23, 24] in which two oscillators (or oscillatory clusters) are in different amplitude regimes with an order of magnitude difference between them.

The outline of the paper is as follows: in Section 2 we give a non-technical overview of the mechanism of mixed mode oscillations we consider. In Section 3 we present some results on the dynamics near folded nodes, concentrating on the information relevant for MMO's. This section contains the main new result of this paper, namely the estimates of the size of the sectors of rotation. In Section 4 we state some results on the existence of periodic orbits of type 1^s (one large and s small oscillations) and give very rough sketches of the proofs. We also indicate how periodic orbits with other Farey sequences can come about. In Section 5 we present some simulations corroborating the results of Section 4. In Section 6 we indicate how the analysis can be extended to systems with two slow and arbitrarily many fast dimensions. Finally, in Section 7 we present a method for finding mixed mode oscillations in systems with two slow and arbitrarily many fast variables.

2 Mixed mode oscillations in three dimensions

In this section we present expository material on MMO's in three dimensions. More precisely, we consider systems of the form

$$\begin{aligned} \varepsilon \dot{x} &= f(x,y,z) \\ \dot{y} &= g_1(x,y,z) \\ \dot{z} &= g_2(x,y,z)\,, \end{aligned} \tag{2.1}$$

with $x \in \mathbb{R}$ as the fast variable and $(y,z) \in \mathbb{R}^2$ as slow variables. We also consider the fast system, which is equivalent to system (2.1) on the fast time scale $\tau = t/\varepsilon$,

$$\begin{aligned} x' &= f(x,y,z) \\ y' &= \varepsilon g_1(x,y,z) \\ z' &= \varepsilon g_2(x,y,z)\,. \end{aligned} \tag{2.2}$$

The two limits obtained by setting $\varepsilon = 0$ in (2.1) and (2.2), respectively, are known as the *reduced problem* and the *layer problem*. The basic philosophy of geometric singular perturbation theory is to characterize solutions of the full problem using the information on both limiting subsystems. Let $S = \{(x,y,z) \,:\, f(x,y,z) = 0\}$ denote the critical manifold which is the phase space of the reduced problem.

Assumption 1 *The critical manifold S is (locally) a folded surface, i.e. $S = S_a \cup \mathcal{F} \cup S_r$ with attracting branch $S_a := \{(x,y,z) \in S \,:\, f_x < 0\}$, repelling branch $S_r := \{(x,y,z) \in S \,:\, f_x > 0\}$ and fold-line $\mathcal{F} := \{(x,y,z) \in S \,:\, f_x = 0,\ f_{xx} \neq 0\}$*

Without loss of generality, we assume that $f_y|_{p\in\mathcal{F}} \neq 0$ holds locally. It follows by the implicit function theorem that S is locally given as a graph $y = \phi(x,z)$, i.e. $f(x,\phi(x,z),z) = 0$. We use this representation $y = \phi(x,z)$ to define a projection of the reduced system

$$\begin{aligned} 0 &= f(x,y,z) \\ \dot{y} &= g_1(x,y,z) \\ \dot{z} &= g_2(x,y,z) \end{aligned} \tag{2.3}$$

onto S. Implicit differentiation of $f(x,y,z) = 0$ gives the relationship $-f_x\dot{x} = (f_y g_1 + f_z g_2)$. It follows that the reduced problem (2.3) projected onto the (x,z)-plane is given by

$$\begin{pmatrix} -f_x\,\dot{x} \\ \dot{z} \end{pmatrix} = \left.\begin{pmatrix} (f_y\,g_1 + f_z\,g_2) \\ g_2 \end{pmatrix}\right|_{y=\phi(x,z)}. \tag{2.4}$$

Note that the fold-line $\mathcal{F}$ is the locus of singularities of (2.4). We rescale time by the factor $-f_x$, obtaining the *desingularized system* of (2.4):

$$\begin{pmatrix} \dot{x} \\ \dot{z} \end{pmatrix} = \left.\begin{pmatrix} (f_y\,g_1 + f_z\,g_2) \\ -f_x\,g_2 \end{pmatrix}\right|_{y=\phi(x,z)}. \tag{2.5}$$

The local dynamics near $\mathcal{F}$ of system (2.5) can be completely understood. The phase portraits of the reduced problem (2.4) and the desingularized system (2.5) are the same, but the orientation of the flow has to be reversed on S_r, see Figure 1.

Typically, fold points $p \in \mathcal{F}$ satisfy the normal switching condition

$$(f_y\,g_1 + f_z\,g_2)|_{p\in\mathcal{F}} \neq 0. \tag{2.6}$$

A fold point p satisfying (2.6) is a *jump point* if there exists a trajectory of (2.4) starting at some point q in S_a and ending at p. Jump points play a fundamental role in relaxation oscillations [27].

Under condition (2.6) the reduced system (2.4) becomes unbounded along the fold-line $\mathcal{F}$. Thus trajectories of system (2.1) reaching the vicinity of $\mathcal{F}$ subsequently jump away from the fold, i.e. a fast transition away from the critical manifold S near $\mathcal{F}$ almost parallel to the x-axis occurs. This jumping behaviour near $\mathcal{F}$ is part of the mechanism leading to relaxation oscillations in system (2.1).

Note that away from $\mathcal{F}$ there exist, by Fenichel theory [9, 12], an attracting manifold $S_{a,\varepsilon}$ and a repelling manifold $S_{r,\varepsilon}$, with S_a and S_r as their singular limits. $S_{a,\varepsilon}$ is only locally invariant and trajectories arrive in the vicinity of the fold-line $\mathcal{F}$ after finite time, where the slow flow on $S_{a,\varepsilon}$ is approximately described by the reduced flow (2.4). Then solutions are forced to jump away from the fold. If, after this fast transition away from the fold, a global return mechanism projects the trajectory back onto the attracting manifold $S_{a,\varepsilon}$, then periodic solutions are possible and we obtain relaxation oscillations. This oscillations can be viewed as simple 1^0 patterns of MMO's. For details on relaxation oscillations we refer to [27, 11].

To obtain true MMO's including small amplitude oscillations the reduced flow has to possess a folded singularity. Typically, a folded singularity is an isolated point $p_0 \in \mathcal{F}$ which violates the normal switching condition (2.6). Therefore, a folded singularity is an equilibrium of the desingularized system (2.5). We call p_0 a *folded node, folded saddle, or folded saddle-node* if, as an equilibrium of (2.5), it is a node, a saddle, or a saddle-node.

Remark: There are two very important limits of folded node, called folded saddle-node of type I and folded saddle-node of type II, both of codimension one in the class of systems we consider. A *folded saddle node* of type I occurs when the linearization of (2.5) at p_0 has an eigendirection tangent to $\mathcal{F}$. Note that $\mathcal{F}$ is a nullcline of (2.5), which implies that the corresponding eigenvalue must be 0.[1] The occurence of the 0 eigenvalue explains the use of the term 'saddle-node'. In fact a generic folded saddle-node of type I leads to the birth of a folded node/folded saddle pair.

A *folded saddle node* of type II corresponds to the case when the linearization of (2.5) at p_0 has a zero eigenvalue with the eigendirection transverse to the fold line $\mathcal{F}$. In the unfolding of a folded saddle node of type II an equilibrium passes from the stable to the unstable sheet of the slow manifold. See [26, 28] for more details on folded saddle nodes.

Assumption 2 *The reduced system (2.3) possesses a folded node singularity $p_0 \in \mathcal{F}$, which is defined by the condition*

$$(f_y g_1 + f_z g_2)|_{p_0 \in \mathcal{F}} = 0 \tag{2.7}$$

and by the requirement that the eigenvalues λ_w and λ_s of the linearization of (2.5) at p_0 satisfy $\lambda_w \cdot \lambda_s > 0$. In addition we assume that λ_w and λ_s are negative.

Henceforth we assume that Assumptions 1 and 2 hold for (2.1) respectively (2.2).

Canards are special trajectories which play a very important role in the dynamics near a folded node. Their defining characteristic is that they originate in $S_{a,\varepsilon}$, continue to the vicinity of the fold, and subsequently, instead of jumping along the fast direction, continue to $S_{r,\varepsilon}$. In geometric terms, a canard corresponds to the intersection of the manifolds $S_{a,\varepsilon}$ and $S_{r,\varepsilon}$ extended by the flow to the vicinity of the folded singularity. Canards are not unique because the corresponding invariant manifolds $S_{a,\varepsilon}$ and $S_{r,\varepsilon}$ are not unique (but exponentially close). For a fixed choice of the invariant manifolds we call their intersections *maximal canards*. Each

[1] In general, if a system of differential equations has an equilibrium with an eigendirection tangent to one of the nullclines then the corresponding eigenvalue must be 0.

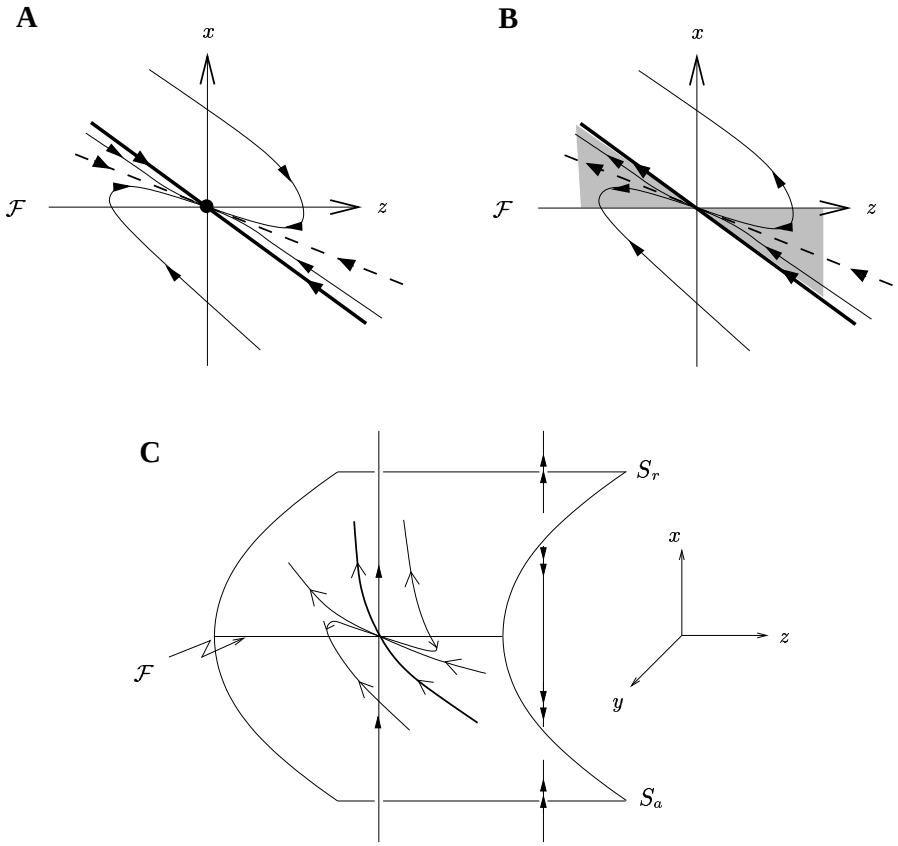

Figure 1 Folded node, A: the desingularized flow, the bold resp. dashed line corresponds to the strong resp. weak eigendirection of the singularity, B: the reduced flow with the singular funnel (shadowed region), C: the reduced flow on the critical manifold S

maximal canard defines a family of canards nearby which are exponentially close to the maximal canard. *Singular canards*, or *canard candidates* are trajectories of the reduced flow (2.4) which pass at p_0 from S_a to S_r. For a folded node there exists a whole sector of singular canards, see Figure 1. Canards existing for (2.1) for $\varepsilon > 0$ arise as perturbations of singular canards. Their number depends in an intricate way on the parameter $\mu = \lambda_w/\lambda_s$ [28]. (we assume WLOG that $|\lambda_w| < |\lambda_s|$). Two of the maximal canards, called the primary canards, are perturbations of the eigendirections of λ_w and λ_s of the desingularized system (2.5). The primary canard corresponding to the eigendirection of λ_w is called the *weak canard* and the primary canard corresponding to the eigendirection of λ_s is called the *strong canard*. It was shown in [28] that near a folded node singularity the trajectories of system (2.1) originating close to the singular funnel enter a region near the fold where they rotate about the weak canard. The rotational property and the existence of the weak canard can be explained purely by a geometric argument. The strong canard can be thought of the locus of a change in the relative position of $S_{a,\varepsilon}$ and $S_{r,\varepsilon}$. The trajectories originating in $S_{a,\varepsilon}$ to one side of the strong canard are trapped by $S_{r,\varepsilon}$ and have to return towards $S_{a,\varepsilon}$. This causes the small rotations and the weak

canard can be understood as the center of rotation. The trajectories originating in $S_{a,\varepsilon}$ to the other side of the strong canard are prevented by $S_{r,\varepsilon}$ from returning to $S_{a,\varepsilon}$ and must follow a fast direction. We refer to the region of rotation as the *funnel*. During their passage near the funnel the trajectories are initially attracted to the weak canard and later repelled from it. The trajectories which enter the funnel are trapped for a significant amount of time, however this behavior is transient and eventually the trajectory exits the vicinity of the fold by jumping along the fast direction. If, after the jump away, a global return mechanism projects this trajectory back onto $S_{a,\varepsilon}$ within the area of attraction of the funnel, then MMO patterns of type 1^s are possible, i.e. periodic solutions consisting of one large amplitude oscillation due to the global return mechanism and s small amplitude oscillations due to the funnel near the folded node singularity.

We would like to describe MMO's in their singular limit. Note that for small $\varepsilon > 0$ fast jumps are executed near the folded node singularity. In the singular limit we describe all these jumps as a projection along the fast fiber of the layer problem through the folded node onto a possible other attracting critical manifold where the trajectory then follows the local reduced flow until it may reach another fold where it gets projected back along another fast fiber onto the original attracting manifold. Cubic shaped critical manifolds are a prominent example which lead to this return mechanism and they are ubiquitous in chemical and biological applications. With that description of the fast jumps we can define a singular limit of MMO's:

Assumption 3 *There exists a singular periodic orbit $\Gamma = \Gamma_a \cup \Gamma_g$ for system (2.1) which consists of a smooth segment Γ_a on S_a within the singular funnel with the folded node singularity p_0 as endpoint. Γ_g represents a global return mechanism onto S_a which has to be specified.*

Theorem 2.1 *Given system (2.1) under Assumption 1-3.*

1. *There exist mixed mode oscillations of type 1^s. It is possible to calculate the maximal number of small oscillations s.*
2. *If the segment Γ_a of the singular periodic orbit Γ consists of a segment of the boundary of the singular funnel (the strong canard) then more complicated MMO patterns of type $L^{s'}$, $L \geq 1$ and $s' \leq s$, are possible.*

Figure 2 shows the basic mechanism to obtain MMO's. In the following we discuss the local and the global aspects to obtain MMO patterns in more detail. We define a return map $\Pi : \Sigma^- \to \Sigma^-$, where Σ^- is a cross section orthogonal to the x-axis away from the fold, such that for small ε, all trajectories under consideration which are projected back onto $S_{a,\varepsilon}$ onto the neighbourhood of the funnel intersect Σ^- (see Figure 3). We decompose this map into $\Pi := \Pi_G \circ \Pi_L$, where $\Pi_L : \Sigma^- \to \Sigma^+$ defines the (local) map near the folded critical manifold, and $\Pi_G : \Sigma^+ \to \Sigma^-$ defines the (global) map defined by the global return mechanism. We begin our analysis with the map Π_L.

3 Small amplitude oscillations – the folded node

The map $\Pi_L : \Sigma^- \to \Sigma^+$ captures the dynamics near the folded singularity where canard solutions exist. Recall that canard solutions are trajectories originating on $S_{a,\varepsilon}$, passing through the neighborhood of a folded singularity, and ending up in $S_{r,\varepsilon}$ where they remain for a considerable amount of time. In [28] the existence of *primary and secondary canards* (see Figure 6) due to a folded node singularity

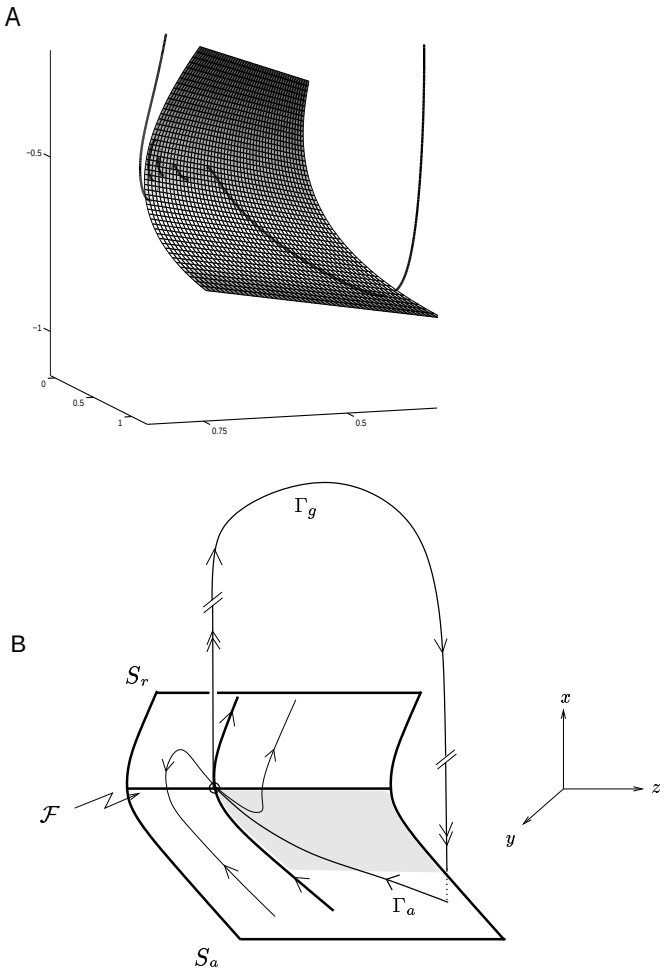

Figure 2 The basic mechanism to generate MMO patterns: A folded node singularity (B: black circle) forms a singular funnel (B: shadowed region). A trajectory Γ_a which enter this funnel makes small amplitude oscillations near the folded node singularity. After leaving the funnel the trajectory may jump away along a fast direction. A global return mechanism (Γ_g) injects the trajectory back into the funnel forming a periodic solution with a 1^s MMO pattern.

was shown as well as rotational properties of solutions near the folded singularity. In the following we analyse these small amplitude oscillations in more detail.

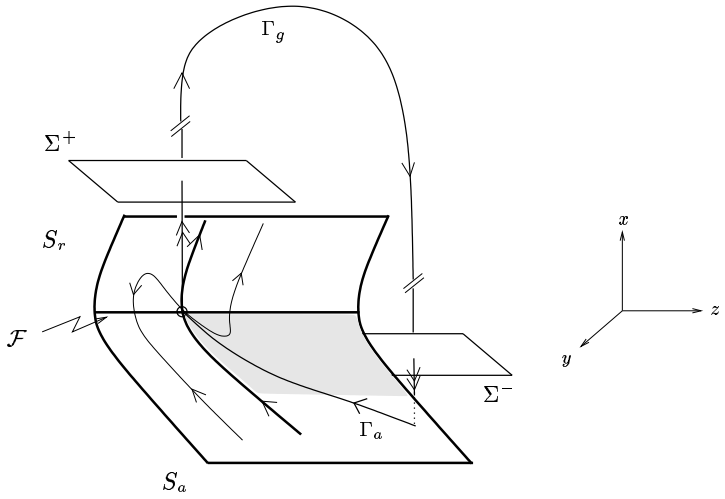

Figure 3 Cross sections Σ^- and Σ^+ to analyse MMO patterns.

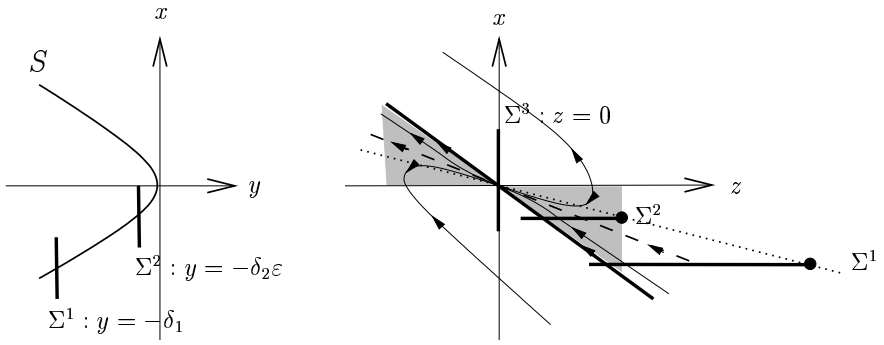

Figure 4 Left: cross-sections Σ^1 and Σ^2 near the fold; Right: projection of reduced flow onto (x, z) plane. Note that the projection of the intersection of the cross-section Σ^1 with the invariant manifold S is one-dimensional. Σ^1 intersects the line of turning points (dotted line). Therefore Σ^1 is just a cross section of the reduced flow to the left of the intersection (black dot) where the flow is directed towards the fold. The same argument holds for the definition of the cross section Σ^2.

Remark: Note that due to the existence of canards the map $\Pi_L : \Sigma^- \to \Sigma^+$ may not be well defined. In the following analysis it will become clear which restrictions have to be made to define the map Π_L well.

Fenichel theory in its classical form guarantees the existence of the slow manifolds $S_{a,\varepsilon}$ and $S_{r,\varepsilon}$ $O(1)$ away from the fold. Thus we define a map $\Pi_1 : \Sigma^- \to \Sigma^1$ where Σ^1 is a cross section defined by $y = -\delta_1$, $\delta_1 > 0$ small, parallel to the fast fibers and $O(1)$ away from the fold. Note there is a natural restriction for Σ_1 to be a cross section due to the folded node. As shown in Figure 4, the flow in a neighbourhood of a folded node has turning points (shown as a dotted line) with respect to z , i.e. the vector field at turning points is parallel to the z-axis. Therefore

Σ^1 may be just well defined as a cross section on a certain interval I_z of z. But this interval I_z always covers the area between the two eigendirections of the folded node (shown as bold and dashed lines) which becomes important in the following analysis.

We next turn to the flow of trajectories past the folded node. We introduce normalizing coordinates which brings system (2.1) into a canonical form near a folded node singularity given by

$$\begin{aligned} \varepsilon\dot{x} &= y + x^2 + O(x^3, x^2z, xyz, \varepsilon) \\ \dot{y} &= -(\mu+1)x - z + O(y, \varepsilon, (x+z)^2) \\ \dot{z} &= -\frac{\mu}{2}, \qquad \mu \in (0,1). \end{aligned} \tag{3.1}$$

Remark: System (3.1) can be seen as one possible normal form near a folded node. The limit $\mu \to 0$ gives the folded saddle-node type II. In [28] a similar normal form of the folded node was studied which has a folded saddle-node type I as its limit for $\mu \to 0$. The results on folded nodes are the same for both normal forms, just the limiting behavior of the folded saddle-nodes is different. Therefore all results on folded nodes obtained in [28] are valid for system (3.1).

The critical manifold S of system (3.1) is a parabolic cylinder with the fold-line $\mathcal{F}$ given by the z-axis and the folded singularity p_0 is at the origin. The reduced system for (3.1) is

$$\begin{aligned} -2x(1+O(x,z))\dot{x} &= -(\mu+1)x - z + O((x+z)^2) \\ \dot{z} &= -\mu/2 \end{aligned} \tag{3.2}$$

and the desingularized system is

$$\begin{aligned} \dot{x} &= -(\mu+1)x - z + O((x+z)^2) \\ \dot{z} &= \mu x + O(x^2, xz)\,. \end{aligned} \tag{3.3}$$

The origin is an equilibrium of node type with eigenvalues $\lambda_s = -1$ and $\lambda_w = -\mu$. Thus $\mu = \lambda_w/\lambda_s \in (0,1)$ defines the ratio between the strong and the weak eigenvalue of the folded node. The phase portraits of the reduced system (3.2) and the desingularized system (3.3) are equivalent to those shown in Figure 1.

We are studying the map $\Pi_f : \Sigma^1 \to \Sigma^+$ induced by the flow of system (3.1). To analyse this map past the folded node we have to introduce intermediate (singular) cross-sections which are sections used in the blow-up analysis of the folded node in [28]. We want to avoid technicalities in this paper and therefore will not introduce the blow-up analysis, but refer for details to [28].

To understand the flow past the fold-line we have to rescale system (3.1) by setting

$$x = \sqrt{\varepsilon}\bar{x}, \quad y = \varepsilon\bar{y}, \quad z = \sqrt{\varepsilon}\bar{z}, \quad t = \sqrt{\varepsilon}\bar{t}. \tag{3.4}$$

Equations (3.1) transform to

$$\begin{aligned} \bar{x}' &= \bar{y} + \bar{x}^2 + O(\sqrt{\varepsilon}) \\ \bar{y}' &= -(\mu+1)\bar{x} - \bar{z} + O(\sqrt{\varepsilon}) \\ \bar{z}' &= -\frac{\mu}{2}, \end{aligned} \tag{3.5}$$

where $'$ denotes $d/d\bar{t}$. System (3.5) is a zoom of the vector field near the folded node singularity. Note that the section Σ^1 is given by $\bar{y} = -\frac{\delta_1}{\varepsilon}$ in system (3.5). We introduce a section $\Sigma^2 : \bar{y} = -\delta_2$, with sufficiently large $\delta_2 > 0$, and define the map $\Pi_2 : \Sigma^1 \to \Sigma^2$.

Remark: Σ^2 is given by $y = -\delta_2\varepsilon$ in the original system (3.1). Similar to Σ^1, the section Σ^2 is just a cross section for a certain interval $I_{z'}$ of z which covers the area of the strong and the weak eigendirection of the folded node. Under the reduced flow (3.2) the interval I_z of Σ^1 is mapped into the interval $I_{z'}$ of Σ^2 (see Figure 4). Therefore the map Π_2 is well defined.

For $\bar{y} < -\delta_2$, it was shown in [28] that system (3.5) has still a normally hyperbolic structure and Fenichel theory can be applied. More specifically, the manifold $S_{a,\varepsilon}$ given by classical Fenichel theory in section Σ^1 can be extended up to the section Σ^2 by the flow of (3.5). Since the extended manifold is an invariant manifold of (3.5) we denote it by $S_{a,\sqrt{\varepsilon}}$. A manifold $S_{r,\sqrt{\varepsilon}}$ is obtained analogously, except by going backwards in time. The following result holds:

Proposition 3.1 [28] *For system (3.5) with $\varepsilon \neq 0$ and also for (3.1) the sets $S_{a,\sqrt{\varepsilon}}$ and $S_{r,\sqrt{\varepsilon}}$ are smooth locally invariant normally hyperbolic manifolds and $O(\sqrt{\varepsilon})$ smooth perturbations of S. The flow on $S_{a,\sqrt{\varepsilon}}$ (respectively on $S_{r,\sqrt{\varepsilon}}$) is an $O(\sqrt{\varepsilon})$ perturbation of the reduced flow.*

Remark: Proposition 3.1 is an extension Fenichel theory up to $O(\sqrt{\varepsilon})$ from the fold $\mathcal{F}$ (which corresponds to $O(\varepsilon)$ in the y direction). In fact it can be proved by application of invariant manifold theory in suitable coordinates [26]. Therefore, the map Π_2 can be completely described by Fenichel theory.

Henceforth we focus on $S_{a,\sqrt{\varepsilon}}$ and $S_{r,\sqrt{\varepsilon}}$ in the coordinates $(\bar{x}, \bar{y}, \bar{z})$ of system (3.5). The advantage of the 'blown-up' system (3.5) is that we can take now the limit $\varepsilon \to 0$ and obtain sets S_a and S_r which are locally invariant for $\{(3.5), \varepsilon = 0\}$. The sets S_a and S_r can be seen as the approximations of $S_{a,\sqrt{\varepsilon}}$ and $S_{r,\sqrt{\varepsilon}}$ at the $O(\sqrt{\varepsilon})$ level. In the following we want to understand how S_a and S_r behave beyond Σ^2. One important property is that S_a, respectively S_r, consist of solutions of $\{(3.5), \varepsilon = 0\}$ of at most algebraic growth as $\bar{t} \to -\infty$, respectively $\bar{t} \to \infty$. In fact these manifolds approach the parabolic cylinder $\bar{y} = -\bar{x}^2$ for $\bar{t} \to \pm\infty$. Furthermore, the unperturbed system $\{(3.5), \varepsilon = 0\}$ has two explicitly known polynomial solutions $\varphi_w(\bar{t})$ and $\varphi_s(\bar{t})$:

$$\varphi_w(\bar{t}) = \left(\frac{\mu}{2}\bar{t},\ -\frac{\mu^2}{4}\bar{t}^2 + \frac{\mu}{2},\ -\frac{\mu}{2}\bar{t}\right)$$

$$\varphi_s(\bar{t}) = \left(\frac{1}{2}\bar{t},\ -\frac{1}{4}\bar{t}^2 + \frac{1}{2},\ -\frac{\mu}{2}\bar{t}\right)$$

We refer to $\varphi_w(\bar{t})$ and $\varphi_s(\bar{t})$ as *singular canards* in the context of the rescaled variables (3.4) and the corresponding system $\{(3.5), \varepsilon = 0\}$. Recall that we defined *singular canards* for (2.4) as solutions that continue from S_a to S_r. Furthermore, $\varphi_w(\bar{t})$ and $\varphi_s(\bar{t})$ are related to the strong and weak eigendirection of the folded node (these are obtained by projecting $\varphi_w(\bar{t})$ and $\varphi_s(\bar{t})$ onto the (x, z) plane). The solutions $\varphi_w(\bar{t})$ and $\varphi_s(\bar{t})$ play a very important role in understanding the properties of $S_{a,\sqrt{\varepsilon}}$ and $S_{r,\sqrt{\varepsilon}}$ beyond Σ^2.

Proposition 3.2 [26] *Consider (3.5) with $\varepsilon = 0$. The invariant sets S_a and S_r are smooth 2 dimensional submanifolds with a common boundary, given by $\varphi_w(\bar{t})$. They have first order contact along $\varphi_w(\bar{t})$ if $(1/\mu) \notin \mathbb{N}$ and higher order contact at $\varphi_w(\bar{t})$ if $(1/\mu) \in \mathbb{N}$. In addition there is at least one intersection, given by $\varphi_s(\bar{t})$. This intersection is transverse for every $\mu \in (0,1)$.*

Remark: It is clear that $\varphi_w(\bar{t})$ and $\varphi_s(\bar{t})$ are both contained in S_a and in S_r (see Figure 4). However the fact that $\varphi_w(\bar{t})$ is the common boundary of S_a and S_r is not immediately clear and requires an additional estimate. Later in this Section we will develop some technical tools which will enable us to sketch the proof of this result.

By a standard application of the Implicit Function Theorem each transverse intersection of S_a and S_r perturbs to a transverse intersection of $S_{a,\sqrt{\varepsilon}}$ and $S_{r,\sqrt{\varepsilon}}$, which corresponds to a maximal canard solution. Thus Proposition 3.2 establishes the existence of the strong canard for any $\mu \in (0,1)$ and the existence of the weak canard for non-resonant μ.

We now consider additional intersections of S_a and S_r. Note that the manifolds S_a and S_r rotate around the singular weak canard. These rotations happen on a compact domain. Rotational properties of the tangent bundles along the weak canard ϕ_w can be inferred from the properties of the solutions of the Weber equation $v'' - tv' + v/\mu = 0$. More specifically, the following holds.

Proposition 3.3 [28] *Given system (3.5) with $\varepsilon = 0$ and $n - 1 < 1/\mu < n$, the invariant manifolds S_a and S_r twist $(n - 1/2)$ times around the primary weak canard in the neighbourhood of the folded node singularity, where a twist corresponds to a half rotation of $180°$.*

Let Σ^3 be a cross section of the flow of (3.5) defined by $\bar{z} = 0$. Note that intersection points of the curves $S_a \cap \Sigma^3$ and $S_r \cap \Sigma^3$ are in one-to-one correspondance with solutions along which S_a and S_r intersect. In the resonant cases $1/\mu \in \mathbb{N}$, the curves $S_a \cap \Sigma^3$ and $S_r \cap \Sigma^3$ have higher order contact at $\phi_w(0)$. Odd resonances lead to a new intersection point while passage through even resonances leads to no new intersections. Wechselberger [28] proves the following result.

Proposition 3.4 [28] *Consider system (3.5) with $\varepsilon = 0$. Suppose that $k > 0$ is an integer such that*

$$2k + 1 < \frac{1}{\mu} < 2k + 3.$$

Suppose in addition that $(1/\mu) \neq 2(k+1)$. Then $S_a \cap \Sigma^3$ and $S_r \cap \Sigma^3$ have k transverse intersection points in addition to $p_s(0)$ and the contact point $p_w(0)$.

Figure 5 shows $2+2$ intersections of $S_a \cap \Sigma^3$ and $S_r \cap \Sigma^3$ of system $\{(3.5), \varepsilon = 0\}$ for $\mu = 0.15$.

Remark: Due to the time reversing symmetry of the unperturbed system $\{(3.5), \varepsilon = 0\}$ given by $T(\bar{x}, \bar{y}, \bar{z}, \bar{t}) = (-\bar{x}, \bar{y}, -\bar{z}, -\bar{t})$ the curves $S_a \cap \Sigma^3$ and $S_r \cap \Sigma^3$ are symmetric images by a reflection across the y axis.

From Proposition 3.4 we conclude

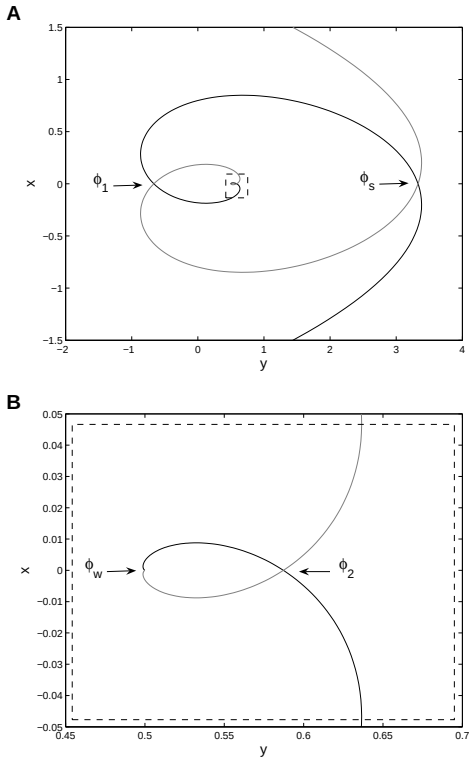

Figure 5 A: The relative position of the manifolds S_a (thin grey curve) and S_r (bold black curve) are shown in section $\Sigma^3 : \bar{z} = 0$ for $\mu = 0.15$, B: zoom of the dashed box area of A. The intersections represent the 2 primary canards denoted as ϕ_w and ϕ_s, as well as 2 secondary canards denoted by ϕ_1 and ϕ_2 predicted by Corollary 3.1. Note, the manifolds rotate around the primary weak canard ϕ_w.

Corollary 3.1 *Under the assumptions of Proposition 3.4 the system (3.1) has, for sufficiently small ε, k secondary maximal canards.*

Remark: The bifurcations of canards for $\varepsilon \neq 0$ are much more complicated than the bifurcations of the unperturbed system, as described in the paragraph following Proposition 3.3 (see [28]). In this paper we assume that μ is not close to resonance, where such bifurcations are of relevance.

We now describe the rotational structure of the secondary canards. For $1/\mu \geq 2k+1$, $k \in \mathbb{N}$ there exist k secondary canards positioned between the two primary canards in section Σ_2. Furthermore, the j-th secondary canard makes $(2j+1)$ twists around the primary weak canard, $1 \leq j \leq k$. The primary strong canard makes also one twist around the primary weak canard. Thus the primary strong canard and the k secondary canards are consecutively separated by a full rotation of 360°. This allows us to define *sectors* in $S_{a,\sqrt{\varepsilon}}$ with distinctive rotational properties bordered by the primary and the secondary canards.

Let $p_j \in S_{a,\sqrt{\varepsilon}}$, $1 \leq j \leq k$, denote the intersection of the j-th secondary canard with Σ^2 and $p_w \in S_{a,\sqrt{\varepsilon}}$, resp. $p_s \in S_{a,\sqrt{\varepsilon}}$, the intersection of the primary

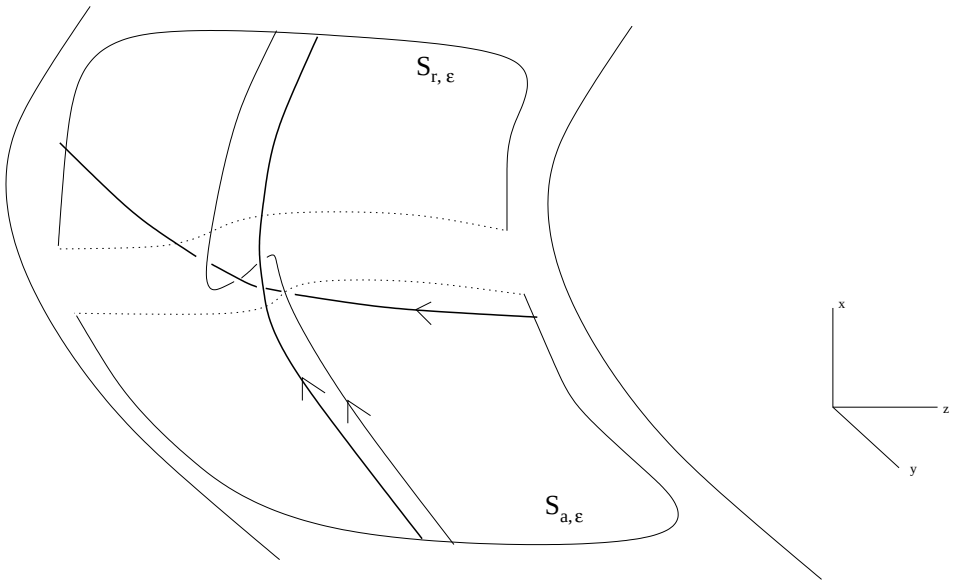

Figure 6 The two primary canards and the first secondary canard

weak canard, resp. strong canard, with Σ^2. Let I_{k+1} be the interval in $S_{a,\sqrt{\varepsilon}} \cap \Sigma^2$ bounded by the end point of $J_{z'}$ close to the weak canard and by p_k. Let I_k be the interval in $S_{a,\sqrt{\varepsilon}} \cap \Sigma^2$ bounded by p_k and p_{k-1}, I_{k-1} the interval in $S_{a,\sqrt{\varepsilon}} \cap \Sigma^2$ bounded by p_{k-1} and p_{k-2}, and so on. Finally, I_1 is the interval bounded by p_1 and p_s. Trajectories with initial conditions in the interior of I_j, $1 \leq j < k+1$, make $(2j + 1/2)$ twists around the primary weak canard, while trajectories with initial conditions in the interior of I_{k+1} make at least $[2(k+1) - 1/2]$ twists around the primary weak canard. All these solutions are forced to follow the *funnel* created by the manifolds $S_{a,\sqrt{\varepsilon}}$ and $S_{r,\sqrt{\varepsilon}}$. After solutions leave the funnel they get repelled by the manifold $S_{r,\sqrt{\varepsilon}}$ and will follow close to a fast fiber in the $\bar{x}$ direction and exit finally through the section Σ^+ given by $\bar{x} = \delta_+/\sqrt{\varepsilon}$ in system (3.5). The singular limit of this fast fiber for the original problem (3.1) is exactly the fiber through the folded node singularity. Note that all these trajectories do not exit through Σ^2.

Remark: The boundaries of the sectors are primary and secondary maximal canards. Consequently, the trajectories close to the boundaries of the sectors will exit consecutively through the sections Σ^2 and Σ^1 near S_r and follow the slow flow near S_r close to the corresponding maximal canard for a certain amount of time before they get repelled and jump away (see Figure 6). Depending on the specific problem under study the position of the exit section Σ^+ may not be suitable, or has to be modified to capture the trajectories passing very close to the boundaries of the sectors.

The remaining part of this section is devoted to estimating the size of the sectors of rotation. More specifically, we continue the secondary canards backwards in time on $S_{a,\varepsilon}$ all the way to the section Σ_1 and ask for the interval size I_j' defined by the canards in Σ_1. The size of the intervals I_j, $1 \leq j \leq k+1$, in the section Σ^2 of system

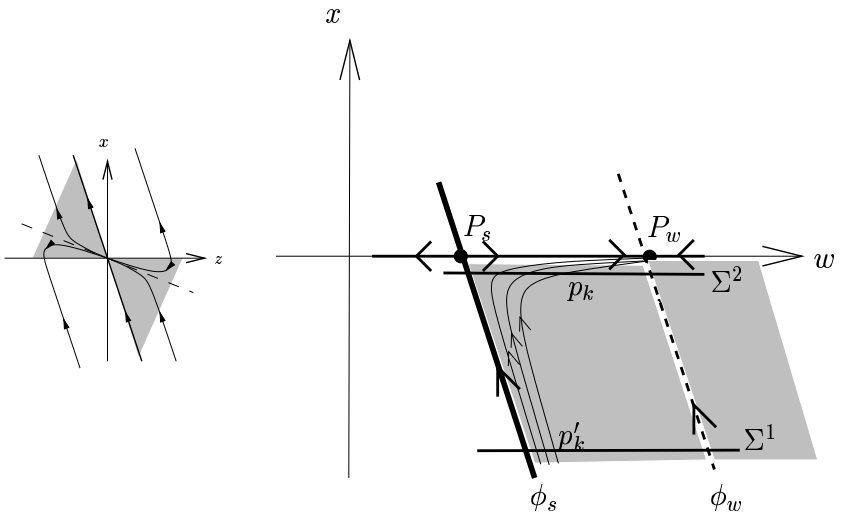

Figure 7 'Blown-up' reduced flow obtained by introducing a new coordinate w=-z/x

(3.5) is $O(1)$, i.e. the primary and secondary canards are all finitely separated. Note that an interval size $O(1)$ in $\Sigma_2 : \bar{y} = -\delta_2$ of system (3.5) becomes an interval size $O(\sqrt{\varepsilon})$ in $\Sigma_2 : y = -\delta_2\varepsilon$ of the original system (3.1).

To estimate the size of the intervals I'_j in Σ^1 we are studying the (inverse) transition map Π_2^{-1} for the reduced flow of (3.2). Since transition maps are independent of time parametrization, we can use the desingularized system (3.3) instead of the reduced system (3.2). In system (3.3) the section Σ^1 is approximately given by $x = -\sqrt{\delta_1}$ and the section Σ^2 is approximately given by $x = -\sqrt{\delta_2\varepsilon}$. To understand the reduced flow close to the node singularity, we introduce a new variable $w = -z/x$. This singular coordinate change unfolds the node singularity and resembles the blow-up analysis done in [26, 28]. In the new coordinates (x, w) the desingularized system (3.3) becomes

$$\begin{aligned} \dot{x} &= -x(\mu + 1 - w + O(x)) \\ \dot{w} &= -(w - \mu)(w - 1) + O(x). \end{aligned} \tag{3.6}$$

Note that the sections $\Sigma^1 : x = -\sqrt{\delta_1}$ and $\Sigma^2 : x = -\sqrt{\delta_2\varepsilon}$ are still the same, but the size of intervals I_j change to $O(1)$ in Σ^2 for system (3.6). Thus, the 'blown-up' desingularized system (3.6) approximates the slow dynamics of the rescaled system (3.5). Looking at the dynamics of (3.6) we find two equilibria: a sink $P_w = (0, 1)$ and a saddle $P_s = (0, \mu)$. The unique attracting eigendirection of the saddle P_s corresponds to the primary strong canard ϕ_s while the incoming attracting eigendirection of the sink P_w corresponds to the the primary weak canard ϕ_w. Thus the 'blow-up' splits the strong and weak eigendirection of the folded node singularity (see Figure 7). We estimate the (inverse) transition time from Σ^2 to Σ^1 and the size of the intervals I'_j in Σ^1 by the linearized system at the equilibrium P_s. The linerization at P_s is given by:

$$\begin{pmatrix} \dot{x} \\ \dot{w} \end{pmatrix} = \begin{pmatrix} -1 & 0 \\ * & (1-\mu) \end{pmatrix} \begin{pmatrix} x \\ w \end{pmatrix}, \tag{3.7}$$

where $*$ is an unspecified term. The estimate of the (inverse) transition time from Σ^2 to Σ^1 for trajectories not close to Φ_w is

$$T = -\ln\sqrt{\varepsilon} + O(1)\,.$$

Next we want to estimate the size of the intervals I'_j, $1 \le j \le k+1$, in Σ_1. It is clear by the phase plane of system (3.6) that all solutions within the sector bordered by the primary canards ϕ_w and ϕ_s are moving towards the strong canard ϕ_s in backward time, because the saddle P_s has the only attracting eigendirection in backward time (see Figure 7). We have an eigenvalue $(\mu - 1)$ corresponding to the attracting eigendirection in backward time along the w-axis of the saddle P_s. We make a linear coordinate change which brings (3.7) for P_s into diagonal form. Then, by solving the equation $\dot{w} = (\mu-1)w$ for $t \in (0, -\ln\sqrt{\varepsilon})$, we can estimate the positions of the points p'_j in Σ^1 corrsponding to the secondary canards ϕ_j. We know that all initial conditions p_j, $1 \le j \le k$, are O(1) away from the equilibrium P_s corresponding to the strong primary canard ϕ_s. We estimate that all points p'_j will be approximately $O(\varepsilon^{(1-\mu)/2})$ close to the strong primary canard ϕ_s in section Σ^1 of system (3.6). By transforming back to the original variables (x, z) the estimate $O(\varepsilon^{(1-\mu)/2})$ for the size of the intervals I'_j holds also for the desingularized system (3.3). We conclude that the following result holds.

Proposition 3.5 *All secondary canards of system (3.1) are $O(\varepsilon^{(1-\mu)/2})$ close to the primary strong canard in section Σ^1.*

Therefore all secondary canards converge to the primary strong canard in the singular limit $\varepsilon \to 0$. Furthermore the sizes of the intervals I'_j for $1 \le j < k+1$ are $O(\varepsilon^{(1-\mu)/2})$ while the size of the interval I'_{k+1} is $O(1)$ because the two primary canards have distance $O(1)$ and therefore $I'_{k+1} = |\phi'_w - \phi'_k| = O(1)$.

Proposition 3.6 *Given system (3.1) and the section $\Sigma^1 : y = -\delta_1$. There exist $(k+1)$ sectors I'_j, $1 \le j \le k+1$, between the two primary canards where k is the number of secondary canards. The size of the sectors I'_j, $1 \le j < k+1$, is $O(\varepsilon^{(1-\mu)/2})$ and the size of sector I'_{k+1} is $O(1)$.*

The qualitative picture is given in Figure 7.

As announced in the paragraph directly following Proposition 3.2 we are now in position to prove that $\phi_w(t)$ is the common boundary of S_a and S_r. More precisely, we prove the following:

Proposition 3.7 [26] *Consider (3.5) with $\varepsilon > 0$. As $\varepsilon \to 0$ the distance between the boundary of $S_{a,\sqrt{\varepsilon}}$ (resp. $S_{r,\sqrt{\varepsilon}}$) and the weak canard converges to 0.*

The idea is that any neighborhood of Φ_w in Σ^1 which does not contain Φ_s is contracted by the flow of (3.6) onto a neighborhood of Φ_w whose size converges to 0 as $\varepsilon \to 0$. This is intuitively clear from Figure 7. More precisely, we prove the following lemma.

Lemma 3.1 *Let I be a closed interval in Σ^1 including the intersection of Φ_w with Σ^1 in its interior but not the intersection of Φ_s with Σ^1. The map Π_2 restricted to I is a contraction with contraction rate $O(\varepsilon^{(1-\mu)/2\mu})$.*

Proof: The procedure is analogous as in the proof of Proposition 3.5 except in forward time. For this reason we need the linearization about P_w, which is given

by:

$$\begin{pmatrix} \dot{x} \\ \dot{w} \end{pmatrix} = \begin{pmatrix} -\mu & 0 \\ * & -(1-\mu) \end{pmatrix} \begin{pmatrix} x \\ w \end{pmatrix} . \tag{3.8}$$

The forward transition time from Σ^1 to Σ^2 for trajectories not close to Φ_s is

$$T = -\frac{1}{\mu} \ln \sqrt{\varepsilon} + O(1) .$$

We now argue, analogously as above, that the evolution of the variable transverse to Φ_w is given approximately by $\dot{w} = (\mu - 1)w$. The required result follows easily. □

Proof of Proposition 3.7: For definiteness let us assume that $p = (x, y, z)$ in $S_{a,\varepsilon} \cap \Sigma_1$ corresponds to the turning point in Σ^1. If p' is the image of p in Σ^2 under the flow of (3.1), then, by Lemma 3.1, p' is $O(\varepsilon^{(1-\mu)/2\mu})$ close to the weak canard (in the (x, w, y) coordinates). This means that p' in the $(\bar{x}, \bar{z}, \bar{y})$ coordinates must be $O(\varepsilon^{(1-\mu)/2\mu})$ close to the weak canard. As the weak canard converges to φ_w as $\varepsilon \to 0$, it follows that p' converges to the intersection point of φ_w with Σ^2. □

4 Global return mechanism and periodic orbits

In this section we state more precise versions of Theorem 2.1 and sketch the proofs. For precise proofs, based on the blow-up method, see our forthcoming article [5].

Recall Assumption 3 postulating the existence of a singular periodic orbit Γ passing through the singular funnel. We now make some additional assumptions on the critical manifold S and on Γ. For simplicity we assume that the critical manifold has S shaped cross-sections. More precisely we assume that S consists of two stable sheets S_1 and S_2, one unstable sheet S_r and two fold lines $\mathcal{F}_1$ and $\mathcal{F}_2$. Let $\mathcal{F}_1'$ (resp. $\mathcal{F}_2'$) be the projection of the fold line $\mathcal{F}_1$ (resp. $\mathcal{F}_2$) onto S_2 (resp. S_1) along the x-direction. We assume that $\mathcal{F}_1$ contains a folded node point and that there is a singular periodic orbit Γ as shown in Figure 8. We make the following assumption:

Assumption 3′ *The orbit Γ_g is defined as*

1. *A critical fiber connecting the folded node point to S_2,*
2. *a (non-singular) trajectory of (3.2) leading to a non-degenerate jump point*
3. *a critical fiber connecting the jump point to $\mathcal{F}_2'$.*
4. *The endpoint of Γ_g is either in the singular funnel or on the strong canard.*
5. *The reduced flow of (3.2) intersects $\mathcal{F}_j'$ transversely at the points $\Gamma \cap \mathcal{F}_j'$, j=1,2.*

Note that Assumption 3′ implies that a singular periodic orbit Γ as shown in Figure 8 exists.

Remark: The results stated below hold not only for an S-shaped return mechanism, but in much higher generality. In fact we only need non-degeneracy assumptions on the singular flow near Γ. However, in the context of this paper we prefer to use the clear and concrete picture given by Assumption 3′.

Remark: If Assumption 3′ does not hold then no MMO's can be expected. We explain this point under the additional assumption that the singular strong canard intersects $\mathcal{F}_2'$ transversely at one point p_s and all points in $\mathcal{F}_2'$ to on side

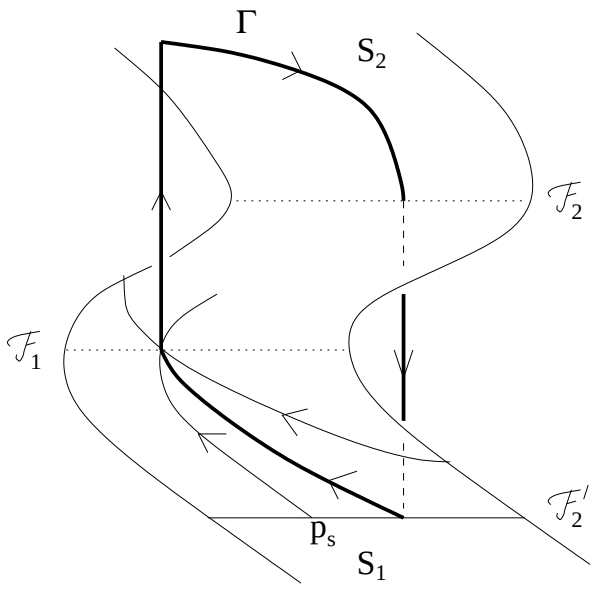

Figure 8 The cubic return mechanism and the singular periodic orbit Γ

of p_s are in the singular funnel (with no further loss of generality we assume that the singular funnel consists of the trajectories under (3.2) of the points in $\mathcal{F}_2'$ to the right of p_s, see Figure 8). Let p_1 be the endpoint of Γ_g and suppose that p_1 is to the left of p_s (see Figure 8). Then, by monotonicity of the reduced flow, the singular trajectory through p_1 must return to $\mathcal{F}_2'$ to the left of p_1, and so on. It follows that no MMO's can exist in this case.

We now present some positive results on the existence of simple MMO's. Recall the rotation sectors I_j', which were defined as intervals in $S_a \cap \Sigma_1$. We will now replace them by exponentially small neighborhoods of I_j' in Σ_1, keeping the same notation. We will make a standing assumption that μ is a a fixed constant between 0 and 1 and not at resonance. We will not make claims about the dependence of the length of I_j' on μ.

Theorem 4.1 *(Existence of* 1^s *MMO) Given system (2.1) under Assumptions 1, 2 and 3'. Assume also the endpoint of* Γ_g *is in the interior of the singular funnel region and not on the weak canard. Then, for sufficiently small* $\varepsilon > 0$*, there exists a stable periodic orbit passing through the sector of maximal rotation* I_{k+1}'.

Sketch of the proof: On the singular level the return map Π maps the entire singular funnel to a single point. It follows that for $\varepsilon > 0$ Π restricted to I_{k+1}' is a very strong contraction. Hence there exists a unique attracting periodic orbit passing through I_{k+1}'. □

Periodic orbits passing through submaximal sectors exist in the unfolding of a codimension one situation. More precisely, we assume that the system depends on a parameter β and variation of β has the effect of moving the the global return point in S_a. We have the following theorem.

Theorem 4.2 *Given system (2.1) under Assumptions 1, 2 and 3'. Assume also that for some $\beta = \beta_0$ the return point is on the strong canard and as β passes through β_0 the return point crosses the strong canard with non-zero speed. Then the following holds provided that ε is sufficiently small:*

For each j there is an interval $\tilde{I}_j$ with length of the order $O\left(\varepsilon^{\frac{1-\mu}{2}}\right)$ such that for each $\beta \in \tilde{I}_j$ there exists a periodic orbit passing through I_j'.

Sketch of the proof: The size of a submaximal sector in $\Sigma^- \cap S_{a,\varepsilon}$ is $O(\varepsilon^{(1-\mu)/2})$. In the vicinity of the fold the sectors are $O(1)$ in the $(\bar{x}, \bar{y}, \bar{z})$ variables, which suggests contraction by factor $O(\varepsilon^{\mu/2})$. From the vicinity of the fold back to Σ^- the sectors do not particularly contract or expand, except for trajectories near the canards. This suggests that the sector may be returned inside of itself and this will happen in the parameter range $\beta = O(\varepsilon^{(1-\mu)/2})$. The resulting map will be a uniform contraction with contraction rate $O(\varepsilon^{\mu/2})$. For the relevant interval of β there will be an attracting periodic orbit passing through the given sector. □

More complicated Farey sequences can occur if no sectors are returned inside themselves. In principle the only restriction is that the number of small oscillations is bounded, but our simulations indicate that only neighboring sectors can interact. The study of more complicated periodic orbits and possible chaos will be the subject of our future work.

Remark: As $\mu \to 0$, which corresponds to an approach to a folded saddle-node, the rate of contraction on the submaximal sectors decreases, in fact our estimate does not imply any contraction in the limit. Also the number of sectors grows indefinitely, while their size decreases to at most $O(\sqrt{\varepsilon})$. In fact most of the sectors in K_2 (the intervals I_j) must shrink to 0 in length as μ approaches 0. This suggests that near a folded saddle-node the dynamics becomes less dissipative, submaximal sectors play a greater role and trajectories visiting many different sectors are more likely to occur.

5 Simulations of MMO's

For our simulations we have used the system:

$$\begin{aligned} \varepsilon \dot{x} &= y + \frac{3}{2}x^2 - x^3 \\ \dot{y} &= -(\mu + 1)x - z \\ \dot{z} &= -\frac{1}{3}(\mu - x + bx^2) \end{aligned} \tag{5.1}$$

Equation (5.1) is a 'van der Pol-like' toy model. There is a folded node point at the origin for any $\mu \in (0, 1)$ and mixed mode oscillations can be observed for a range of b values (b corresponds to β of the preceding section). An important concern was to pick μ sufficiently large relative to ε, in order to stay out of the folded saddle-node range, but not too large, so that the oscillations near the fold could be observed. A good choice of μ and ε turned out to be $\mu = 0.15$ and $\varepsilon = 0.001$. Note that $6 \leq \frac{1}{\mu} \leq 7$, so that our theory predicts the presence of three sectors of rotation, namely I_1', I_2' and I_3'.

The following figures show the time series of the periodic orbits found, corresponding to various cases of the theorems presented above. Note that the evolution of both x and z near the fold consists of oscillation and drift along the weak canard. To eliminate the drift we used $x+z$ as dependent variable. The region of existence of MMO's starts at $b \approx -0.9$ and 1^3 solutions exist for $b \approx -1.25$ or less. For our simulations we chose $b = -1.25$, which is close to the boundary of the sector. For smaller b's the first two rotations become extremely small so that they essentially cannot be seen.

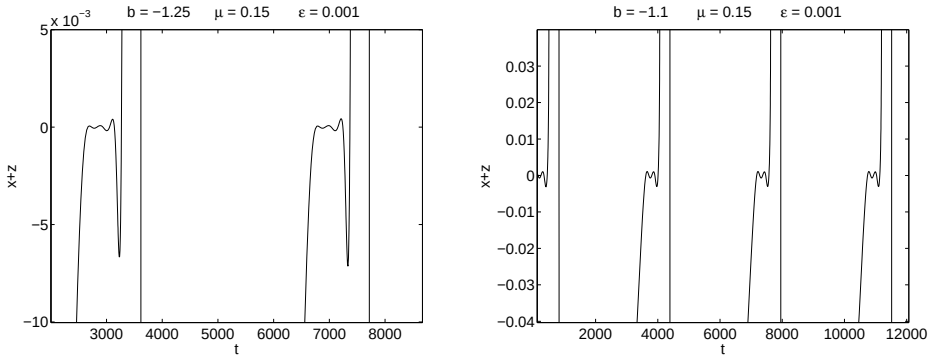

Figure 9 Left: Maximal sector solution MMO 1^3, sector I_3'; Right: MMO 1^2, periodic solution passing through I_2'

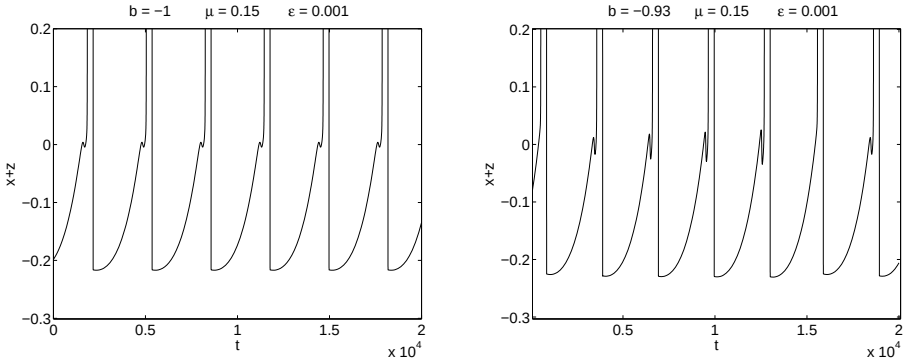

Figure 10 Left: MMO 1^1, periodic solution passing through I_1'; Right: Periodic solution MMO $1^1 1^1 1^1 1^1 1^0$ from the chaotic region

6 More fast dimensions

In this section we extend the theory presented above to the case of two slow and m fast dimensions, with m arbitrary. In this context a fold line is defined by the requirement that the m by m matrix of linearization of the fast equation in the fast directions should have a simple 0 eigenvalue. In this case there exists a local center manifold spanned by the slow variables and the critical direction of the fast variables. The local problem is governed by the flow on the center manifold, which is three dimensional, with one fast and two slow variables. Consequently it is possible to define the sectors of rotation and the funnel analogously as in the preceding sections, and to generalize the requirements on the global return. The results on MMO's in this generalized context are analogous as in the basic case.

A reduction theorem.
Given are equations of the form

$$\begin{aligned} \varepsilon \dot{x} &= f(x,y) \\ \dot{y} &= g(x,y) \qquad \text{with} \quad x \in \mathbb{R}^m,\ y \in \mathbb{R}^2 \end{aligned} \tag{6.1}$$

The above system has two slow and $m \geq 1$ fast variables. Let

$$S_0 = \{(x,y) \ : \ f(x,y) = 0\}$$

be the critical manifold. The following result shows how to obtain a reduction to systems with one fast and two slow variables.

Theorem 6.1 *Assume $(x_0, y_0) \in S_0$ is such that $D_x f(x_0, y_0)$ has a 0 eigenvalue with algebraic multiplicity 1 and all the other eigenvalues are in the left half plane. Then there exists a three dimensional center manifold M with the following properties:*
(1) *M is tangent to the three dimensional space spanned by the slow directions and $(v, 0, 0)$, where v is the nullvector of $D_x f(x_0, y_0)$*
(2) *M is exponentially attracting*
(3) *The vector field (6.1) reduced to M has a fold point of the type studied by Szmolyan and Wechselberger* [26, 28]. *More precisely (6.1) reduced to M has the form:*

$$\begin{aligned} \varepsilon \dot{\sigma} &= \tilde{f}(\sigma, y) \\ \dot{y} &= \tilde{g}(\sigma, y) \qquad \sigma \in \mathbb{R},\ y \in \mathbb{R}^2 \end{aligned} \tag{6.2}$$

with $\tilde{f}_\sigma(0, y_0) = 0$. The point $(\sigma, y) = (0, y_0)$ corresponds to (x_0, y_0).

Proof: The proof is completely analogous to the proof of the existence of a slow manifold. The center manifold M is non-unique, but any M is given as a graph as follows:

$$M := \{(x_0 + \sigma v + \phi(\sigma, y), y), \sigma \in (-\delta_0, \delta_0)\},$$

with δ_0 sufficiently small and $\phi = O(\sigma^2, (y - y_0)^2)$. The function ϕ is as smooth as f and g and if f and g are C^k then the k-jet of ϕ at $(0, 0, y_0)$ is uniquely determined. The functions $\tilde{f}$ and $\tilde{g}$ are defined as follows:

$$\begin{aligned} \tilde{f}(\sigma, y) &= w \cdot f(x_0 + \sigma v + \phi(\sigma, y), y) \\ \tilde{g}(\sigma, y) &= g(x_0 + \sigma v + \phi(\sigma, y), y) \end{aligned} \tag{6.3}$$

and w is the left nullvector of $D_x f(x_0, y_0)$, i.e. $w^T D_x f(x_0, y_0) = (0, 0)$. □

Theorem 6.2 *If, in addition to the assumptions of Theorem 6.1, we assume that*

$$w \cdot D_y f(x_0, y_0) g(x_0, y_0) = 0. \tag{6.4}$$

then the point (x_0, y_0) is a folded singularity in the sense of [26, 28].

Proof: According to [26, 28] system (6.2) has a folded singularity at $(0, y_0)$ if $\tilde{f}_y(0, y_0) \cdot \tilde{g}(0, y_0) = 0$. Clearly this condition is equivalent to (6.4). □

A point p_0 is now a folded singularity of (6.1) if it is contained in M and is a folded singularity of (6.2). Classification of folded singularities is analogous as in 3D.

Global return mechanism.
We assume that (x_0, y_0) is a folded node. The layer problem restricted to the invariant plane $y = y_0$ has saddle node point at x_0 with one center and $m-1$ stable direction. This condition guarantees that the flow on the center manifold for the layer problem restricted to the invariant plane $y = y_0$ approaches $x = x_0$ in one direction and moves away from $x = x_0$ in the other direction. In particular there is a trajectory going away from x_0. We refer to this trajectory as the *unstable critical fiber*. Now the generalization of the global return Γ_g is a sequence of trajectories of the layer flow and the reduced flow, starting with the unstable critical fiber and ending in the stable sheet of S_0 which contains the folded node point. The Assumptions 3 and/or 3' can now be easily generalized and theorems analogous to Theorem 4.2 and Theorem 4.1 hold.

7 Reduced flow and desingularization

In this section we derive a method for finding the desinguarized flow near the fold. The purpose of this is to develop an efficient way of finding folded singularities. Recall that in the basic case of two slow and one fast variables folded singularities are equilibrium points of the desingularized equation (3.3). Suppose for a problem with two slow and m fast variables a suitable generalization of the desingularized equation is available. One can then (possibly numerically) find equilibria and determine whether they correspond to folded singularities. The type of the folded singularity can be deduced from the properties of the linearization of the desingularized equation.

The reduced flow is given by the algebraic system:

$$\begin{aligned} 0 &= f(x, y) \\ \dot{y} &= g(x, y) \qquad \text{with} \quad x \in \mathbb{R}^m,\ y \in \mathbb{R}^2 \end{aligned} \tag{7.1}$$

In order to get a better understanding of the system (6.2) we would like to eliminate the constraint $f(x, y) = 0$. At a hyperbolic point of S_0 we can just solve for y as a function of x. Near the fold this is not possible, but one may be able to solve for either the fast variables x or for one slow variable and one fast variable. We will consider the following two cases:
(i) There exists $i, j \in \{1, \ldots, m\}$, $i \neq j$, such that $D_{(x_i, x_j)} f(x_0, y_0)$ has rank 2.
(ii) $D_{(x_i, y_j)} f(x_0, y_0)$ has rank 2, where $i \in \{1, \ldots, m\}$ and j equals 1 or 2.

The case $D_{(x_i,x_j)}f(x_0,y_0)$ has rank 2.

With no loss of generality we assume that $(i,j)=(1,2)$. We write $x=(\tilde{x},(x_3,x_4,\ldots,x_m))$, with $\tilde{x}=(x_1,x_2)$. Let $(x_3,x_4,\ldots,x_m,y)=\Phi(\tilde{x})$ denote the (possibly locally defined) solution of $f(x,y)=0$. We use $f(x,y)=0$ to derive the following identity:

$$0=\frac{d}{dt}(f(x,y))=D_xf(x,y)\dot{x}+D_yf(x,y)g(x,y)$$

or

$$D_xf(x,y)\dot{x}=-D_yf(x,y)g(x,y). \tag{7.2}$$

Let $C(x,y)$ denote the transpose of the co-factor matrix of $D_xf(x,y)$. We apply $C(x,y)$ to both sides of (7.2), getting

$$\det D_xf(x,y)\dot{x}=-C(x,y)D_yf(x,y)g(x,y). \tag{7.3}$$

Note that we need only two independent equations, namely the ones for $\dot{x}_1$ and $\dot{x}_2$. We have

$$\det D_xf(\tilde{x},\Phi(\tilde{x}))\dot{\tilde{x}}=-P_{(1,2)}C(\tilde{x},\Phi(\tilde{x}))D_yf(\tilde{x},\Phi(\tilde{x}))g(\tilde{x},\Phi(\tilde{x})), \tag{7.4}$$

where $P_{(1,2)}$ is the projection onto the first wo coordinates. For the important case of $m=2$ we have

$$C=\begin{pmatrix}\frac{\partial f_2}{\partial x_2} & -\frac{\partial f_1}{\partial x_2}\\ -\frac{\partial f_2}{\partial x_1} & \frac{\partial f_1}{\partial x_1}\end{pmatrix}$$

and

$$\det D_xf(x,\Phi(x))\dot{x}=-\begin{pmatrix}\frac{\partial f_2}{\partial x_2} & -\frac{\partial f_1}{\partial x_2}\\ -\frac{\partial f_2}{\partial x_1} & \frac{\partial f_1}{\partial x_1}\end{pmatrix}D_yf(x,\Phi(x))g(x,\Phi(x)) \tag{7.5}$$

Remark: If $(x(t),y(t))$ is a trajectory of (7.4) then it is the trajectory of (7.1).

We now rescale the time by $\det D_xf(x,\Phi(x))$ obtaining the reduced and desingularized equation:

$$\dot{\tilde{x}}=-P_{(1,2)}C(\tilde{x},\Phi(\tilde{x}))D_yf(\tilde{x},\Phi(\tilde{x}))g(\tilde{x},\Phi(\tilde{x})). \tag{7.6}$$

For $m=2$ we get

$$\dot{x}=-\begin{pmatrix}\frac{\partial f_2}{\partial x_2} & -\frac{\partial f_1}{\partial x_2}\\ -\frac{\partial f_2}{\partial x_1} & \frac{\partial f_1}{\partial x_1}\end{pmatrix}D_yf(x,\Phi(x))g(x,\Phi(x)) \tag{7.7}$$

Now we have the following proposition:

Proposition 7.1 *An equilibrium (x_0,y_0) of (7.6) is a folded singularity in the sense of Section 6 if $D_xf(x_0,y_0)$ has a zero eigenvalue of algebraic multiplicity* 1.

Proof: We assume for simplicity that $m=2$. In the general case the proof is similar.

If $D_xf(x_0,y_0)$ has a simple eigenvalue 0 then the vector

$$\left(\frac{\partial f_2}{\partial x_2}(x_0,y_0),-\frac{\partial f_1}{\partial x_2}(x_0,y_0)\right)$$

is either 0 or a left eigenvector of $D_xf(x_0,y_0)$. The same holds for

$$\left(-\frac{\partial f_2}{\partial x_1}(x_0,y_0),\frac{\partial f_1}{\partial x_1}(x_0,y_0)\right),$$

namely it is either 0 or a left eigenvector of $D_x f(x_0, y_0)$. It follows that (x_0, y_0) is an equilibrium of of (7.6) if and only if the condition (6.4) holds. □

The case $D_{(x_i,y_j)}f(x_0,y_0)$ has rank 2.
We assume for simplicity that $m = 2$. We also assume, with no loss of generality, that $i = j = 2$, i.e. $D_{(x_2,y_2)}f(x_0,y_0)$ is invertible. We can now find a smooth function Φ so that $(x_2, y_2) = \Phi(x_1, y_1)$. Further we proceed as in the case of two slow and one fast variable obtaining the reduced equation in the following form:

$$\begin{aligned} \dot{y}_1 &= g_1(x_1, y_1, \Phi(x_1, y_1)) \\ \frac{\det D_{(x_1,x_2)}f}{\det D_{(x_2,y_2)}f}\dot{x}_1 &= g_2(x_1, y_1, \Phi(x_1, y_1)) - \frac{\det D_{(y_1,x_2)}f}{\det D_{(x_2,y_2)}f} g_1(x_1, y_1, \Phi(x_1, y_1)). \end{aligned} \tag{7.8}$$

The desingularized flow is given by

$$\begin{aligned} \dot{y}_1 &= g_1(x_1, y_1, \Phi(x_1, y_1))\frac{\det D_{(x_1,x_2)}f}{\det D_{(x_2,y_2)}f} \\ \dot{x}_1 &= g_2(x_1, y_1, \Phi(x_1, y_1)) - \frac{\det D_{(y_1,x_2)}f}{\det D_{(x_2,y_2)}f} g_1(x_1, y_1, \Phi(x_1, y_1)). \end{aligned} \tag{7.9}$$

Acknowledgement: The authors would like to express gratitude to Dr. Horacio Rotstein and Dr. Jonathan Rubin for carefully reading an earlier version of the manuscript.

References

[1] A. Arnéado, F. Argoul, J. Elezgaray and P. Richetti, Homoclinic chaos in chemical systems. *Physica D* **62** (1993) 134-168.

[2] E. Benoit, J-L. Callot, F. Diener, M. Diener, Chasse au canard, *Collect. Math.* **31** (1981), 37-119.

[3] K. Bold, C. Edwards, J. Guckenheimer, S. Guharay, K. A. Hoffman, J. Hubbard, Ricardo Oliva and W. Weckesser, The forced van der Pol equation II: canards in the reduced system. *SIAM Journal on Applied Dynamical Systems* **2** (2003), 570-608.

[4] K.M. Brucks and C. Tresser, A Farey Tree organization of locking regions for simple circle maps, *Proc. Amer. Math. Soc* **124** (1996), 637-647.

[5] M. Brøns, M. Krupa, M. Wechselberger, Folded nodes and mixed mode oscillations, in preparation (2006).

[6] C. T. Dickson, J. Magistretti, M. H. Shalinsky, E. Fransen, M. E. Hasselmo, A. Alonso, Properties and role of I(h) in the pacing of subthreshold oscillations in entorhinal cortex layer II neurons, *J Neurophysiol.* **83** (2000), 2562-79.

[7] Jonathan Drover, Jonathan Rubin, Jianzhong Su, and Bard Ermentrout. Analysis of a canard mechanism by which excitatory synaptic coupling can synchronize neurons at low firing frequencies. *SIAM J. Appl. Math.* **65** (2004), 65-92.

[8] I. R. Epstein, K. Showalter, Nonlinear chemical dynamics: oscillations, patterns, and chaos, *J. Phys. Chem.* **100** (1996), 13132.

[9] N. Fenichel, Geometric singular perturbation theory, *J. Differential Equations* **31** (1979), 53-98.

[10] J. Guckenheimer, K. A. Hoffman and W. Weckesser. The forced van der Pol equation I: the slow flow and its bifurcations. *SIAM Journal on Applied Dynamical Systems* **2** (2003), 1-35.

[11] J. Guckenheimer, M. Wechselberger, L.-S. Young, Chaotic Attractors of Relaxation Oscillators, accepted for publications in *Nonlinearity* (2006).

[12] C.K.R.T. Jones, Geometric singular perturbation theory, in *Dynamical Systems*, Springer Lecture Notes Math. **1609** (1995), 44-120.

[13] M. Koper, Bifurcations of mixed-mode oscillations in a three-variable autonomous van der Pol-Duffing model with a cross-shaped phase diagram, *Physica D* **80** (1995), 72-94.
[14] K. Krischner, M. Eiswirth, G. Ertl, Oscillatory CO oxidation on Pt(110): Modeling of temporal self-organization, *J. Chem. Phys.* **96** (1992), 9161-72.
[15] M. Krupa and P. Szmolyan. Extending geometric singular perturbation theory to nonhyperbolic points – fold and canard points in two dimensions. *SIAM. J. of Math. Anal.* **33** (2001), 286-314.
[16] R. Larter and C. G. Steinmetz. Chaos via mixed mode oscillations. *Phil. Trans. R. Soc. London* **A337** (1991), 241-298
[17] J. Maselko, H. L. Swinney, Complex periodic oscillations and Farey arithmetic in the Belousov–Zhabotinskii reaction, *J. Chem. Phys.* **85** (1986), 6430-41.
[18] G. Medvedev, J. Cisternas, Multimodal regimes in a compartmental model of the dopamine neuron, *Physica D* **194** (2004), 333-356.
[19] A. Milik, P. Szmolyan, H. Loeffelmann, E. Groeller, Geometry of mixed-mode oscillations in the 3d autocatalator, *Int. J. of Bifurcation and Chaos* **8** (1998), 505-519.
[20] C. A. Del Negro, C. G. Wilson, R. J. Butera, H. Rigatto, J. C. Smith, Periodicity, mixed-mode oscillations, and quasiperiodicity in a rhythm-generating neural network, *Biophys J.* **82** (2002), 206-14.
[21] H. G. Rotstein, T. Oppemann, J. A. White, N. Kopell. A reduced model for medial entorhinal cortex stellate cells: subthreshold oscillations, spiking and synchronization, submitted (2005).
[22] H. G. Rotstein, N. Kopell, A. Zhabotinsky, I. R. Epstein, A canard mechanism for localization in systems of globally coupled oscillators, *SIAM J. Appl. Math*, **63** (2003), 1998-2019.
[23] H. G. Rotstein, N. Kopell, A. Zhabotinsky, I. R. Epstein, Canard phenomenon and localization of oscillations in the Belousov-Zhabotinsky reaction with global feedback, *J. Chem. Phys.* **119** (2003), 8824-8832.
[24] H. G. Rotstein, R. Kuske, Localized and asynchronous patterns via canards in coupled calcium oscillators, accepted for publication in *Physica D* (2006).
[25] M. Schell, F. N. Albahadily, Mixed-mode oscillations in an electrochemical system. II. A periodic-chaotic sequence, *J. Chem. Phys.* **90** (1989), 822-828.
[26] P. Szmolyan, M. Wechselberger, Canards in $\mathbb{R}^3$, *J. Differential Equations* **177** (2001), 419-453.
[27] P. Szmolyan, M. Wechselberger, Relaxation Oscillations in $\mathbb{R}^3$, *J. Differential Equations* **200** (2004), 69-104.
[28] M. Wechselberger, Existence and Bifurcation of Canards in $\mathbb{R}^3$ in the Case of a Folded Node, *SIAM J. Appl. Dyn. Sys.* **4** (2005), 101-139.
[29] A. M. Zhabotinsky, Periodic kinetics of oxidation of malonic acid in solution, *Biofizika* **9** (1964), 306-311.